INFN note xx/yy/zz 19th May 2002
INFN Sezione di Genova

Update on the *EUSO* photo-detector design

M. Ameri[(a)], S. Cuneo[(a)], F. Fontanelli[(a,b)], V. Gracco[(a,b)], P. Musico[(a)], M. Pallavicini[(a)], A. Petrolini[(*,a,b)], F. Pratolongo[(a)] and M. Sannino[(a,b)].

a) INFN, Sezione di Genova, Via Dodecaneso 33, I-16146 Genova, Italy
b) Dipartimento di Fisica dell'Università di Genova, Via Dodecaneso 33, I-16146 Genova, Italy

Abstract

This report updates the status of the development of some critical items of the EUSO photo-detector, at the time of the beginning of ESA phase A. The items discussed includes the design of focal surface layout, the MAPMT base-board and micro-cell, the photo-detector modules and volume, mass and power budgets.

*) Corresponding author; e-mail: `Alessandro.Petrolini@ge.infn.it`

Contents

1 Introduction

The present document is an update of the following previous documents and presentation at EUSO Collaboration and technical meetings:

- V. Gracco and A. Petrolini, Use of multi-anode photo-multipliers for the AirWatch photon detector, 23 October 1998, AirWatch technical note, available at the EUSO Genova Web site http://www.ge.infn.it/euso/;
- Study report on the EUSO photo-detector design, Report INFN/AE-01/04, available at http://wwwsis.lnf.infn.it/pub/INFN/AE-01/04.pdf, 06/04/2001;
- M. Ameri et al., 01/06/2001, Proc. 27th ICRC (2001): EUSO (Extreme Universe Space Observatory): the focal surface photo-detector, available at http://www.ge.infn.it/euso/docs/icrc2001-paper.pdf;
- Presentation at the Annecy EUSO Collaboration meeting, 02/10/2001, available from LiveLink;
- Informal memo for the EUSO Focal Surface (FS) subgroup, circulated in October 2001;
- Presentation at the Paris EUSO Collaboration meeting, 28/02/2002, available from LiveLink.

The various updates are based on the progressive availability of additional and/or more precise input data required for a correct photo-detector (PD) design.

It must be stressed that many critical information required for the PD design is totally missing, while other information is available in a form that requires some post-processing or, in some case, some guesses. In some cases this prevents, for the time being, to draw firm conclusions on many aspects. A summary of the most critical required information will be reported later.

1.1 Definitions

As far as the technical and engineering aspects are concerned, the overall PD on the FS must be considered one, single (and complex) instrument. Its different components must be considered within the global economy of the overall PD. Therefore the PD is meant to include the following elements:

- the sensors;
- the optical adapters (light collection systems);
- the front-end, trigger and data-handling electronics;
- the focal surface layout, structure and engineering, its integration with the EUSO structure;
- the interfaces between the different components;
- all the ancillary systems required for the proper operation and control of the photo-detector.

2 The *EUSO* photo-detector

2.1 General comments

During the EUSO phase A it is mandatory to define a realistic, even if not final, arrangement for the EUSO photo-detector, and to demonstrate its feasibility, compatibly with the scientific objectives.

Everything may be re-discussed and studied more deeply in phase A. New developments might be accounted for. Everything can be improved later, but today we must show that we have in mind a realistic baseline for the PD, possibly to be improved.

Different options can be allowed, whenever a more detailed study is required to assess their characteristics.

The detailed PD design requires precise input data from the optics. This is especially true for the layout of the FS in order to perform the fine-tuning of the geometry. Therefore only when these precise and complete input data will be available the precise design of the PD layout can be made. This explains while some approximations have been done in the present studies but the detailed fine-tuning has not been carried on, yet.

2.2 The sensor

We proposed to use commercial MAPMT, R5900/R7600 series, for an AirWatch-like photo-detector in 1998 as the most (or, probably, the only) viable option, at that time. This device is also being used in the AMS experiment, committed to fly on the Shuttle and to be installed in the ISS a long time before EUSO. Many critical items have been faced since then, and realistic solutions were discussed and proposed, based on the existing or just perceived constraints. Recently a new evolution of the R7600 MAPMT, the R8520, has become available, with a much larger sensitive area (about $24 \times 24\,\mathrm{mm}^2$) obtained by introducing a weak focusing between the photo-cathode and the first dynode. Actually only the 16 channels version is available. Some increase in the number of pixels is foreseen by Hamamatsu (25 or 36), but, apparently, not up to 64, because the cross-talk would be too high. The new R8520-M16F, with 16 channels, has therefore a 6 mm pixel size and one might also expect a comparatively larger region with low efficiency between each pixel. The new R8520-M16F is very appealing, but some critical issues must be checked quickly to assert the suitability. Among these the following items must be mentioned.

- Uniformity of the sensitive area, cross-talk, aging effects and space qualification issues (mainly structural).
- The weak focusing implies a large gap (much larger than R7600): the effects of magnetic fields (longitudinal and transverse) on gain and efficiency must be checked. The much more compact R7600 starts to loose efficiency for applied magnetic fields of the order of 10 gauss. The use of a magnetic shield would be difficult due to the large range of incidence angles of the photons on the FS.
- From Yoshi Takahashi document on the optics (10/2001): one cm on the FS corresponds to a $0.23°$ angle. If one assumes a reasonable minimum distance between MAPMTs equal to 27 mm, then the R8520-M16F plus the RIKEN optical adapter gives a pixel size, at the edge, of 7.5 mm, corresponding to $0.17°$. It must be carefully studied whether such a large pixel size, compared to previous assumptions, is compatible with the physics requirements.
- Physics and full detector simulation must define the maximum acceptable pixel size. This requires, necessarily, at least a simplified detector simulation.

If the optics spot size turns out to be too big, compared to the physics requirements, one should use smaller pixels on the PD to improve the position determination by applying statistical methods. It must be stressed that some MAPMT packing schemes might require a minimum MAPMT distance larger than 27 mm, which might be difficult to recover by means of an optical adapter.

Finally before relying too much on new sensors one has to be careful, and keep in mind, for instance, the Flat Panel PMT saga. The standard MAPMT R7600 is a device on the market since many years. Its characteristics have steadily improved with time thanks to feedback from end-users to the manufactures and thanks to the improvements of the production processes.

Many conclusions about the layout are actually independent on the choice M16/M64/M16F version, as all these versions have about the same physical transverse dimensions and mass, while the M16F is a few mm longer than M16/M64. Clearly the use of a 16-channels version (with a total number of channels reduced by a factor four) will help to save on mass, power, design and realization complexity).

In case of use of the M16F one might probably save on the mass of the optical adapter. An optical adapter would be probably required in any case, to recover the residual dead region at the edges and the one introduced by the required MAPMT clearance in a realistic close packing. Anyway this would be certainly simpler, due to the smaller demagnification factor required.

2.3 Angular segmentation of the PD

It is a common feeling that an angular segmentation of $\Delta\alpha \approx 0.15°$, corresponding to $\Delta L \approx 1$ km at the Earth is enough for the physics objectives of EUSO. Anyway one should check this by using a realistic PD design, with its holes, inefficiencies, optical image quality degradation, signal degradation and also including the simulation of all the sources of background and noise as well as stray light. This goal has to be reached before the end of phase A, to guide the PD design. In previous estimates the 64 channels version has been used just because this is the option that produces the maximum possible segmentation of the FS and the most challenging design.

2.4 The optical adapters

A detailed report about possible light collection systems will be distributed as a separate note.

2.5 Optics and PD layout

The following, standard and provisional, parameters for the optics and FS will be assumed.

- Lens Diameter: LD = 2.5 m;
- f-number: $f/\# = 1.25$;
- Entrance pupil diameter: $D_{\mathrm{EP}} = 2.0$ m;
- FoV: $\gamma = 30°$;
- Maximum radius of the FS: $r_{\mathrm{MAX}} = 1.13$ m;
- Focal surface area: 4.41 m^2.

The FS shape is deduced from Yoshi note. The tabular form of the data requires fitting or interpolation. The data are well fitted, to within 0.3 mm, by a polynomial of degree seven. A fit to a paraboloid provide a fit to the data to within 7 mm. The residuals of the difference between the points and the paraboloid show four zero-crossings. This means that the optics FS has a rather wavy shape. A parabolic fit will be assumed with $z \sim \alpha r^2$ with $\alpha = 0.290\,\mathrm{m}^{-1}$ and $r_{\mathrm{MAX}} = 1.13$ m. When a more precise and complete information on the optics will be available this will be taken into account.

Two comments are in order about the Yoshi note (October 2001):

- rounding errors are not negligible from the table: they are greater that 0.23°, i.e. much larger than the expected optics resolution;
- edge effects are significant: the last point is in fact clearly anomalous as a result, probably, of its location at the very edge of the interval; this point has then to be taken with some caution.

Note that detailed information on the spot size and depth of focus, very critical items for the PD design, is missing.

2.5.1 The depth of focus of the optics

Note that, even if the depth of focus appears to be rather large (a few mm can be apparently tolerated) one should be rather tight on the fitting to the FS because there are other unavoidable facts whose effect has to be minimized by relying on the depth of focus. The alignments of the FS with the main optics as well as their distance, for instance, are critical items. Preliminary estimates indicate that a relative rotation of the optics and the FS up to one degree and an uncertainty in the absolute distance up to three mm has to be foreseen. The defocusing produced by these effects sum to the intrinsic PD defocusing. Another factor which adversely affects the spot size is the slicing of the main Fresnel lenses, which will be most probably required to support the large and thin lenses. The alignment and stability of the positioning of the different pieces will affect the spot size making it worse.

2.6 FS and optical sensors positioning

The average directions of the light rays falling onto the focal surface of an optical system are not necessarily perpendicular to the focal surface itself. Therefore, when filling the focal surface with light sensors, one has to face two competing requirements: the need to follow as closely as possible the focal surface shape (to avoid defocusing effects), and the need to align the input window of the sensor (supposed to be flat) perpendicularly to the average direction of the incident rays (to maximize the solid angle coverage of the sensors with respect to the average direction of the incident rays, thus minimizing the required number of sensors).

However the light rays reach any point on the focal surface converging toward the point itself (to within the spot size). Therefore any rotation of the sensor input window with respect to the focal surface necessarily introduces shadowing of one sensor to the neighboring ones (i.e. optical image quality degradation) and light rays hitting the insensitive side of the sensors (i.e. light losses).

A safe way to get a predetermined geometrical acceptance is to fill the focal surface with sensors having the input windows coincident with the focal surface (actually tangent to it). This might not be cheap, in term of the number of sensors required, if the light rays reach the focal surface with an average direction very different from the local normal, as the sensor input window are rotated with respect to the average direction of the light rays and the solid angle coverage is not the maximum possible. However this approach does not introduce image quality degradation (due to defocusing), nor shadowing from neighboring sensors nor photons hitting the side walls of the sensors (lost or, possibly, generating stray light). This is, in a sense, the natural positioning of the sensors.

A second alternative might be used, under very specific circumstances. If the light rays are very inclined with respect to the local normal to the focal surface and if the rays reach the focal surface almost parallel to each other (i.e. large $f/\#$-number of the main optics), an arrangement with the sensor input window perpendicular to the incident rays average direction might be cheaper. In fact it allows to use a smaller number of sensors without significant defocusing effect nor light rays hitting the sides of the sensors nor shadowing effects due to the almost parallel incident rays directions.

2.7 FS layout basic philosophy

The following guidelines were assumed for the FS layout design, trying to take into account not only the requirement to collect as much light as possible but also to collect it in a useful way, by introducing, as far as possible, the minimum degradation of the image quality provided by the optics. It was also attempted to take into account the overall engineering design of the PD and the space qualification issues, as far as we can understand today, within the presently perceived constraints and based on the information available as of today. Note that, a priori, a PD module is something different from a (logical) macro-cell (defined for the trigger). They can be coincident, if that is useful.

- Simplify the design as much as possible. After a reasonable design has been done, any update of the design to increase the performance, will be compared to increase of complexity, difficulty, cost, manpower as well development and realization time.

- Design, as far as possible, a modular system, physically as well as logically. Modularity helps for many aspects, including: fault propagation limitation, independence of the different modules, spare modules procurement, as well as development and design.

- Design a layout with some symmetry, possibly matching the overall EUSO structure (six-fold or eight-fold, probably) and some kind of pattern replication. This will help all the EUSO realization phases by reducing the number of different items to design, prototype, test, realize and have available as spares.

- Realize a good fit to the ideal FS: no more than a few mm discrepancy can be tolerated. In fact, due to the large incidence angles of the photons on the FS the depth of focus is necessarily limited. An approximate estimation can be done starting by the usual relation:

$$\Delta w \approx \Delta z \tan\theta_\gamma \qquad \Longrightarrow \qquad \overline{\Delta w} \approx 0.3\Delta z \tag{2.1}$$

  where Δz is the displacement of the FS in the average direction of the incident photons, Δw is the displacement perpendicular with respect to the average direction of the incident photons (approximately parallel to the tangent plane to the FS) and θ_γ is the angle of incidence with respect to the average direction of the incident photons. One can assume very naively, for all the photons, $\tan\theta_\gamma \approx 0.3$, by taking into account the optics f-number. As a result one obtains that a displacement of the FS of one cm corresponds to a an average shift in the transverse direction of three mm, which corresponds to the radius of the monochromatic spot size.

- Optimize the filling factor of the FS at the edge of FoV: more events are detected there coming from a larger distance from EUSO and suffering a larger atmospheric attenuation. A bad performance at the edge of FoV might actually end up in a reduced effective EUSO FoV.

- Try to have a good fraction of well-reconstructed EAS. As a non-flat FS cannot be tessellated without holes by square flat devices (i.e. the actual MAPMTs) one has probably to accept in any case some loss of acceptance. In this case it is preferable to have a subset of events well reconstructed, instead of having the inefficiencies smeared on all events.

The angular granularity is determined by the MAPMT and MAPMT pitch, assuming to use a suitable optical adapter to demagnify the 27 mm onto the sensitive MAPMT area. In the case of M16F the RIKEN optical adapter is assumed, which produces different size pixels (larger at the edges). One then obtains the following values, where the minimum values correspond to the smaller pixel (only apply to M16F) at the EUSO nadir, while the maximum values correspond to the larger pixel (only apply to M16F) at the edge of the EUSO FoV.

2.8 FS geometry basics

The angular granularity is fixed by the MAPMT, with a suitable optical adapter, according to the following table 2.8

M16	$\Delta\alpha \simeq 0.15°$	$\Delta x_E \simeq 1.0$ km $\div$ 1.3 km
M64	$\Delta\alpha \simeq 0.08°$	$\Delta x_E \simeq 0.5$ km $\div$ 0.7 km
M16F	$\Delta\alpha \simeq 0.17°$	$\Delta x_E \simeq 1.2$ km $\div$ 1.5 km

To follow as closely as possible the symmetry properties of the FS, a surface of rotation, the layout will be made with a number of rings, running like the parallels on the FS.

In all the proposed layouts the maximum estimated distance of the sensors from the ideal FS is kept below a few mm. In case one uses the M16/M16F, the larger pixel size might allow larger modules for the same amount of defocusing. The defocusing, however, rises as the square of the module side. In fact for a given local radius of curvature of the FS, R, and rectangular module of sides a and b, with $L = \sqrt{a^2 + b^2}$, the maximum discrepancy is given by the relation:

$$\Delta z \simeq 0.5 \cdot R \left[1 - \sqrt{1 - L^2/(4R^2)}\right] (\simeq L^2/(16R) \qquad \text{if } L \ll R) \qquad . \tag{2.2}$$

Another important item is given by the probability that an EAS of a given length on the FS will completely fall inside a given region. Assuming rectangular modules of sides a and b, the approximate probability that any EAS, of length l, starting inside the module is fully contained inside the same module, is given by:

$$\text{Prob} \approx 1 - \frac{(a+b)\,l}{a\,b} + \frac{9\,l^2}{4\,a\,b} \qquad l < a/2,\ l < b/2 \tag{2.3}$$

2.9 FS engineering

The packing of the devices has to be optimized to reduce losses in the geometrical acceptance, due to dead regions between the close packed devices, and defocusing effects, originating from a positioning of the sensor at some distance from the ideal focal surface. This makes the mechanical assembly difficult.

A modular structure is preferred. The overall structure might consist of small functional units (elementary cells) assembled in larger modules. The elementary module consists of a limited number of MAPMTs sharing some common resource like being installed on the same PCB base-board, having one common HV power supply and/or voltage divider, a common magnetic or electric screen (whenever required), common heat dissipation facilities and all of the front-end electronics plus as much as possible of the readout electronics integrated in the module.

The elementary cells can be thick multi-layered Printed Circuit Boards (PCB). A number of these modules, each one making an essentially autonomous system, are then put together to make a module. These are independent structures tied to each other by a common support structure and having a shape determined by the layout of the focal surface.

MAPMTs are therefore assumed to be packed in 2×2 elementary units, called micro-cells. A realistic MAPMT pitch is assumed to be 27.0 mm to account also for the large tolerances on the MAPMT dimensions provided by Hamamatsu (± 0.5 mm).

The micro-cell concept is useful because, in addition to introducing a modular structure, it allows sharing, of many resources, between MAPMTs, such as PCBs, HV/LV, MAPMT voltage divider, cables and connectors and electronic chips. This sharing improves the economy and make design, production and testing easier.

It will be assumed that a module is made of an array of close-packed MAPMTs with a suitable shape, possibly surrounded by a border of variable thickness running all around the MAPMTs, to leave space for the mechanics of the module. Due to the packing of the modules the distance among the modules is much larger than one mm at some places among the borders. This will help the engineering as far as fixation of the modules is concerned. Of course the detailed design of the module geometry requires the final fine-tuning of the geometry.

In principle, we might want to optimize the PD granularity as a function of the location of the FS, according to the optics spot size, thus using different devices in different places.

3 Some possible layouts

Based on the assumptions and guidelines described above a few possible layouts were proposed. For most of them a preliminary engineering functional design was carried on.

The idea was to start from very simple layouts, to estimate their performance. After doing that, the layout was made more and more complex to increase the geometrical acceptance at the price of increased complexity. Complexity would manifest itself in an increase of manpower requirements, development time and money, for instance if many different components (e.g. modules) have to be realized.

At a certain point the Collaboration will have to decide how much it is worth paying to increase the geometrical acceptance (i.e. the number of collected events) by a few percent. The few percent of evens to recover will have a much larger cost per event than the others.

Note that, due to the reasons mentioned above about the impossibility to make a precise fine-tuning of the geometry without a reasonably defined design of the optics, some points are just an approximation. The major one is the lack of tuning of the maximum angular coverage of the layouts, which is just approximate. Another one is the fact that the positioning of the modules on the ideal FS, quite a difficult task if one wants to minimize the defocusing effects, was just an approximate one. Anyway the geometry and depth of focus will allow a precise fine-tuning. The precise determination of the geometry also requires a realistic mechanical design of the components.

3.1 Layout six-fold symmetric with all the modules identical

It is based on all identical 6×6 MAPMTs or 8×8 MAPMTs modules. The characteristics of the 6×6 and a drawing are summarized below. The filling factor is only 0.81 and the coverage is particularly poor at low FoV. It is clear that a large part of the loss could be recovered, in principle, by filling the holes between modules with triangular modules. It is also clear that the coverage at low FoV can be improved by using smaller modules Note that the central polygon might be either a special module or just removed.

```
Number of modules in row is            :   {     6.,     12.,     18.,     24.,     30.,     36.}
Base module dimension                  :   { +164.0, +164.0, +164.0, +164.0, +164.0, +164.0}
Starting from angle                    :   {   +3.2,    +6.3,    +9.5,   +12.8,   +16.0,   +19.3}
Ending at angle                        :   {   +6.1,    +9.4,   +12.7,   +16.0,   +19.2,   +22.5}
Required ending angle                  :     +23.410
Total number of modules                :   126
Total number of sensors                :   4536
Sensor filled area                     :      +3.307
Filling factor                         :      +0.806
Filling factor central polygon         :      +0.017
Paraboloid's area up to coverage ($m^2$):      +4.102
```

For this layout a full simulation of the expected geometrical acceptance confirms the expectations.

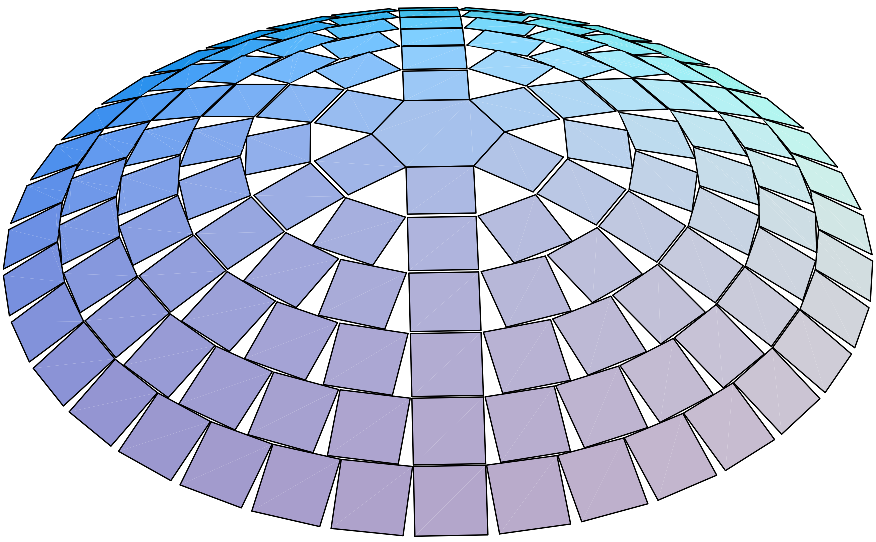

3.2 Layout six-fold symmetric with modules of two different sizes

The simplest variation on the previous theme is by allowing smaller modules at small FoV, to try to improve the performance where it is bad. The improvement in the filling factor is modest but, at least, the holes at small FoV are smaller.

```
Number of modules in row is            :   {     6., 12., 18., 24., 30., 18., 24., 30., 36.}
Base module dimension                  :   {+82.0,+82.0,+82.0,+82.0,+82.0,+164.0,+164.0,+164.0,+16
Starting from angle                    :   {  +1.6,+3.1,+4.8,+6.4,+8.0,+9.7,+12.9,+16.2,+19.5}
Ending at angle                        :   {  +3.0,+4.7,+6.3,+7.9,+9.6,+12.8,+16.1,+19.4,+22.7}
Required ending angle                  :     +23.410
Total number of modules                :   198
Total number of sensors                :   4698
Sensor filled area                     :      +3.425
Filling factor                         :      +0.824
Filling factor central polygon         :      +0.004
Paraboloid's area up to coverage ($m^2$):      +4.157
```

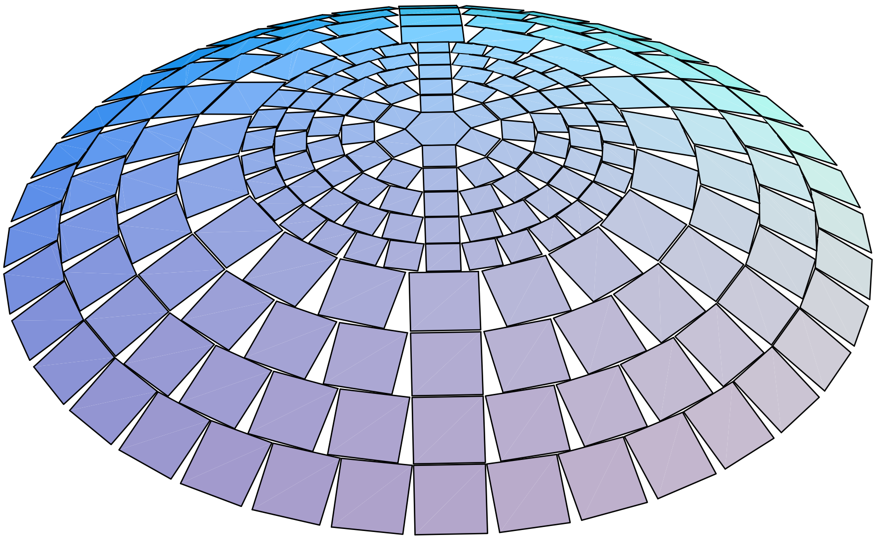

3.3 Layout based on trapezia

Starting form the previous layouts one can change the modules to a trapezium with one side perpendicular to the two basis. In this way the loss of acceptance due to the filling of the trapezium with square section MAPMTs, is only present on one side of the trapezium. However, to get the maximum filling, one has to chose smaller modules at small FoV and therefore two different module sizes are required, each one coming in three slightly different variations (i.e. different major basis). Note that the main losses come from the inefficient filling of the MAPMTs inside the trapezium at the inclined side. Now the filling factor goes up to 0.88.

```
Number of modules in row is            :  {     6., 12., 18., 12., 18., 24., 30., 36.}
Base module dimension                  :  { +82.0,+82.0,+82.0,+164.0,+164.0,+164.0,+164.0,+164.0}
Starting from angle                    :  {   +1.6, +3.1, +4.8, +6.5, +9.8, +13.0, +16.2, +19.5}
Ending at angle                        :  {   +3.0, +4.7, +6.3, +9.6, +12.9,+16.2, +19.4, +22.7}
Required ending angle                  :    +23.410
Total number of modules                :   156
Total number of sensors                :  5040
Sensor filled area                     :     +3.674
Filling factor                         :     +0.879
Filling factor central polygon         :     +0.004
Paraboloid's area up to coverage ($m^2$):     +4.179
```

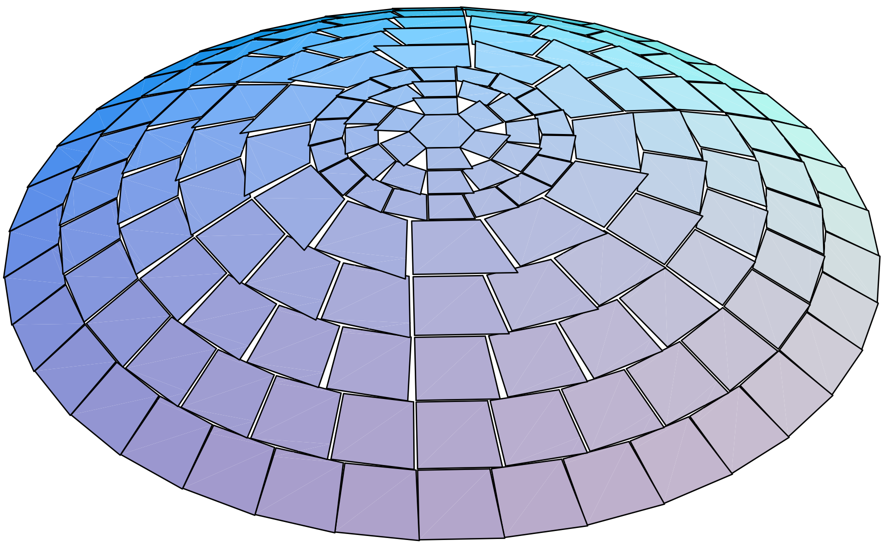

3.4 A 2×2 MAPMTs, micro-cell based layout

One can try to improve the filling factor even more by using square modules made of four MAPMTs (i.e. the module coincide with the micro-cell). The filling factor rises to 0.92. Note that in this case the gap between modules is very small and therefore a modified RIKEN optical adapter might recover that loss. The coverage of the FS is more uniform. Of course the mechanics might turn out to be more complicated.

3.4.1 Direct installation on the FS support

One possibility would be the direct installation of the modules on the FS support. However this approach removes one level of modularity (i.e. the PD modules) which must be then re-introduced, in any case, at least for the electronics (trigger).

3.4.2 Installation based on PD modules

One, probably more interesting solution, would be to define a larger supporting PD module to hold the micro-cells. This might be viewed, in a sense, as using large modules with micro-cells distributed, instead of being packed in a square array, as it is supposed in the layouts described in the previous sections. In other words the supporting module is shaped as required by the micro-cells layout, the orthogonal approach compared to the previous layouts, when the module structure was defined before and the filling with micro-cells followed after. The symmetry of the layout should make the choice of the geometry of the module quite simple. In this case the micro-cells are all identical and, therefore the architecture is simple, but one would need a few different kind of support modules. These support modules would then be the only items that need to be done in different shapes. The natural drawback is that, by using large support modules, the fitting to the FS becomes worse as compared to the excellent fitting of a single micro-cell installation, assuming that the supporting module is flat. This option is, anyway, very interesting.

```
Number of modules in row is            :   {     6., ==>>, 126.}
Base module dimension                  :   { +54.0 }
Starting from angle                    :   {   +1.0, ==>>, +22.3}
Ending at angle                        :   {   +2.0, ==>>, +23.4}
Required ending angle                  :     +23.410
Total number of modules                :   1386
Total number of sensors                :   5544
Sensor filled area                     :      +4.042
Filling factor                         :      +0.918
Filling factor central polygon         :      +0.002
Paraboloid's area up to coverage ($m^2$):     +4.402
```

For this layout a full simulation of the expected geometrical acceptance confirms the expectations.

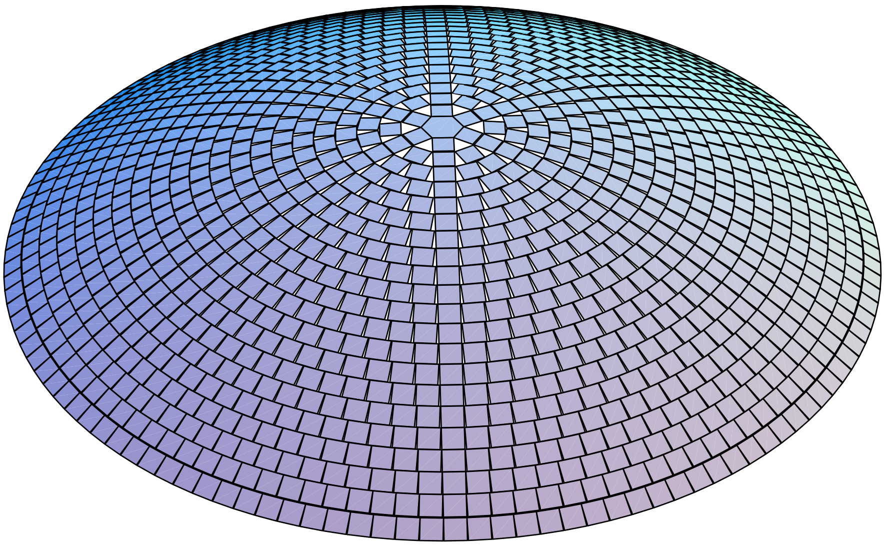

3.5 A single MAPMT based layout

If one accepts to get rid of the micro-cell concept one finally arrives at a single MAPMT installation. While the filling factor rises up to 0.93 the engineering is certainly more complex as the micro-cell concept, and the economy that it carries, have been lost. As in the case of layout defined in section **??** the two different sub options might apply here with the same comments as before:

- direct installation on the FS support (as in 3.4.1);
- installation based on PD modules (as in 3.4.2).

```
Number of modules in row is            :   {     6., ==>>, 258. }
Base module dimension                  :   {  +27.0 }
Starting from angle                    :   {   +0.5, ==>>, +22.9}
Ending at angle                        :   {   +1.0, ==>>, +23.4}
Required ending angle                  :     +23.410
Total number of modules                :   5676
Total number of sensors                :   5676
Sensor filled area                     :      +4.138
Filling factor                         :      +0.935
Filling factor central polygon         :      +0.000
Paraboloid's area up to coverage ($m^2$):      +4.426
```

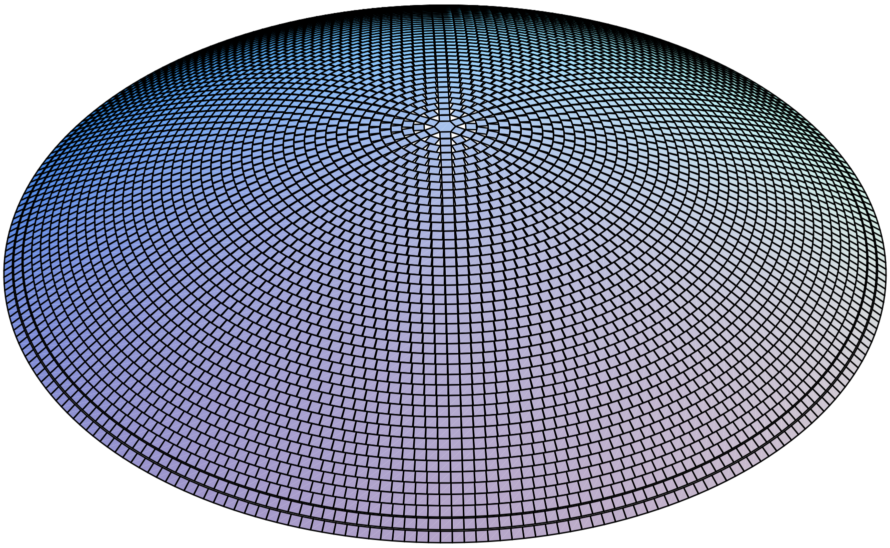

3.6 Conclusions on the FS layout

The required goodness of the coverage of the FS has to be defined as a trade-off with the feasibility, manufacturability and simplicity of the realization and relative implications on cost, developing and realization times.

The simplest layout (section ??),based on modules all identical between each other, allows just a ≈ 0.8 filling factor, with rather large holes, especially at low FoV. Its basic design has been shown already and demonstrated to be feasible.

If the coverage is not considered good enough one must accept more complex arrangements, with their implications in terms of increase of complexity, difficulty, cost, manpower as well development and realization time.

A more complex layout, providing a much better performance, is the one based on micro-cells (section ??) or the one based on a single MAPMT installation (section ??). In this case the PD modules are built according to the optimized layout of the micro-cells or single MAPMTs.

Note that in both cases an additional complexity increase can improve the filling factor even more. In fact the optical adapter, which will be most probably required, whatever the final choice of the MAPMT, can be easily shaped in such a way to recover some part of the small dead areas between, respectively, micro-cells or MAPMTs. This can be accomplished by slightly changing the shape of the light collection system from the square to a slightly deformed trapezoidal shape. Assuming that this can recover a full coverage on the, respectively, micro-cell or MAMPT, one has to take into account that some clearance between different light collection systems will be required for mechanical reasons. The light collection system is assumed to be integrated with the, respectively, micro-cell or MAMPT and therefore the clearance is required only between different, respectively, micro-cells or MAPMTs. The limiting coverage which can be reached by this approach can be estimated by the relation:

$$\varepsilon_{\mathrm{FILLING}} \simeq 1 - \frac{Np\delta}{2A_{\mathrm{coverage}}} \qquad , \tag{3.1}$$

where δ is the minimum allowed clearance between different, respectively, micro-cells or MAPMTs, p is the perimeter of the micro-cells or MAPMTs and A_{coverage} is the total area covered by the specified layout and N is the number of micro-cells or MAPMTs of the layout. One thus finds, assuming $\delta = 0.5$ mm:

$$\text{micro-cell based layout} \quad \Longrightarrow \quad \simeq 0.983 \tag{3.2}$$

$$\text{MAPMT based layout} \quad \Longrightarrow \quad \simeq 0.965 \quad .. \tag{3.3}$$

Note that the loss in the single MAPMT layout is exactly twice the one of the single micro-cell layout because, for the given assumptions, the former has exactly twice the dead areas of the latter due to the clearance between light collection systems. This is basically due to the fact that, for a given clearance, the sensitive to dead area ratio improves as the basic unit becomes larger.

Note that a different symmetry pattern (e.g. 8-fold symmetry) might be considered. Anyway, just by chance, it turns out that the 6-fold symmetry is most suitable to have a coverage with large filling factor. In fact any symmetry pattern imposes constraints on the layout (on the number of elements per ring) and the dimensions of the MAPMTs and micro-cells as well as the geometry of the FS are such that the 6-fold symmetry allow filling of the FS with a good coverage.

4 The micro-cell base-board

The micro-cell (elementary cell) consists of:

- the sensors;
- the base-board, a thick PCB housing all the other components;

- the voltage dividers;
- the front-end electronics chip;
- the connectors for HV/LV, signal and controls;
- the optical adapter;
- any other required structural or functional element (e.g. components required to help heat transfers away from the micro-cell).

The design of the micro-cell base-board has been described elsewhere (see the references).
The micro-cell was conceived with the following guidelines in mind.

- To allow close packing of the MAPMTs with a precise relative positioning.
- To build a compact module with different functionalities integrated onto the base-board. The base-board acts as the structural element, housing the MAPMTs, front-end electronics, and all the other required components, including the paths to carry the signals from the MAPMTs to the front-end electronics and to the outside of the base-board and the components to deal with the heat generated on the base-board.
- To allow a sharing of different resources between different MAPMTs:
  - one common mechanical supporting structure;
  - voltage dividers common to different MAPMTs and common HV/LV power connections;
  - common electro-mechanical components such as cables, connectors, heat bridges, etc.;
  - one common front-end electronic chip: in case the 16-channel MAPMT will be used one common (64-channel) chip is foreseen, while in case of use of the 64-channel MAPMT a 256-channel chip might be difficult to realize.
- To be a single, self-contained and autonomous system, designed as a general purpose instrument to be used in other applications.

The underlying idea is to have the maximum possible close-packing between the MAPMTs in order to reduce the non-sensitive areas on the FS.

The base-board is fixed, along two orthogonal axis at the center, to the PD module supporting back-planes, by means of screws and dowel pins. This allows a precise relative positioning of the different micro-cells onto the PD module. The base-board is fixed on the back-plane supporting structure of the PD module by means of two dowel pins and screwed by means of two steel screws. Screws and pins fit into metallized holes drilled into the PCB. They also act as thermal bridges to convey the heat generated on the base-board away from it, to the PD module. High accuracy, conventionally available, should allow the precise positioning of the micro-cells, so that the design characteristics can be kept without any interference during assembly and dismounting operation. The location of the holes on the PCB will be a compromise between the structural requirements and electrical layout.

As any micro-cell is totally autonomous and it is individually fixed to the PD module supporting back-planes, one has a complete flexibility in the choice of the shape of the PD module, including, possibly allowance for a curved shape.

The signals from the MAPMT anodes are carried on the back-side of the thick base-board where they can be either extracted by means of high-density connectors (0.5 mm pitch), or carried to a front-end chip housed on the back-side of the base-board.

The MAPMT side of the base-board also houses the components of the voltage dividers to power the dynode chain. Up to one voltage divider per MAPMT (i.e. four in total) can be housed onto the base-board (as it is in the prototype). Alternatively one might install only one or two voltage dividers.

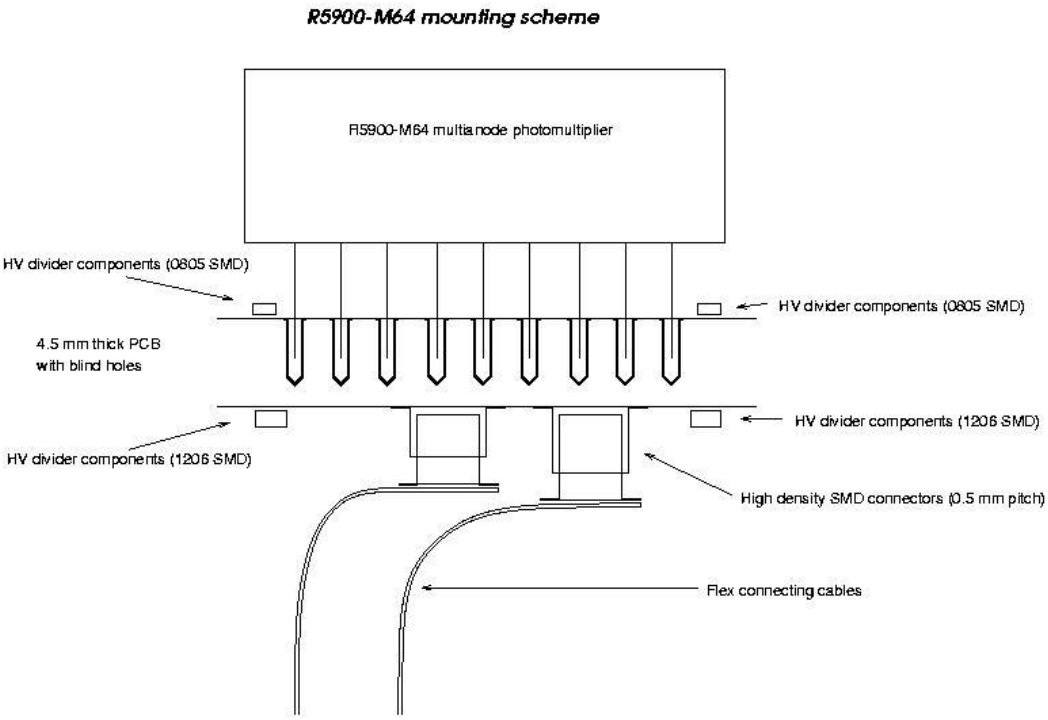

Figure 1: View of the cross-section of the first prototype version of the base-board.

The thick base-board includes a copper layer, 0.5 mm thick, to help to drain away from the base-board the heat by conduction, through screws, pins and, possibly, dedicated heat bridges.

A schematic view of the cross-section of the base-board is shown in figure 1.

A prototype was developed to be used in laboratory tests: its front and back side in a laboratory setup are shown in figure **??**. In the actual design the back-side houses eight high-density connectors. In the final design the front-end chip is supposed to be housed there.

4.1 Micro-cell structural analysis

A preliminary FEA simulation of the base-board was carried on, modeling the base-board and the four MAPMTs installed on it, i.e. all the significant masses of the whole micro-cell but the optical adapters. The optical adapters were not modeled due to the large uncertainty on the real optical adapter design. The modal analysis has determined a first modal frequency of 588 Hz, which can be easily eliminated by changing the constraint scheme, compatibly with the base-board layout. Anyway this first mode, due to friction, is expected to be damped. The second mode, at 1183 Hz frequency (whose displacements are shown in figure 2), would become, adding this constraint, the first one.

The system looks pretty stiff. Therefore it is even conceivable to make the base-board slightly thinner, thus saving mass.

4.2 The first version prototype

In the first prototype the MAPMTs were installed onto the PCB by means of a socket integrated into the PCB by means of blind holes. The internal socket was equipped with single pins soldered to the PCB. This explains the rather large thickness of the base-board, which is however useful to provide the required structural strength. The present thickness is 5 mm. This might be slightly reduced,

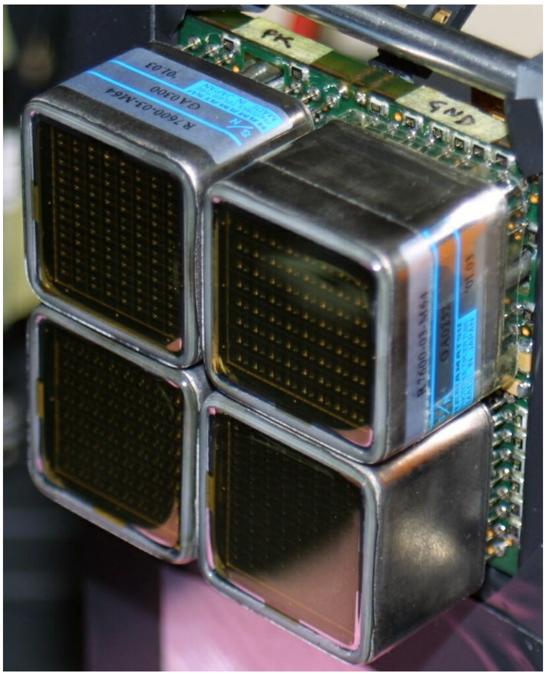

(a) The first base-board prototype: front-side view

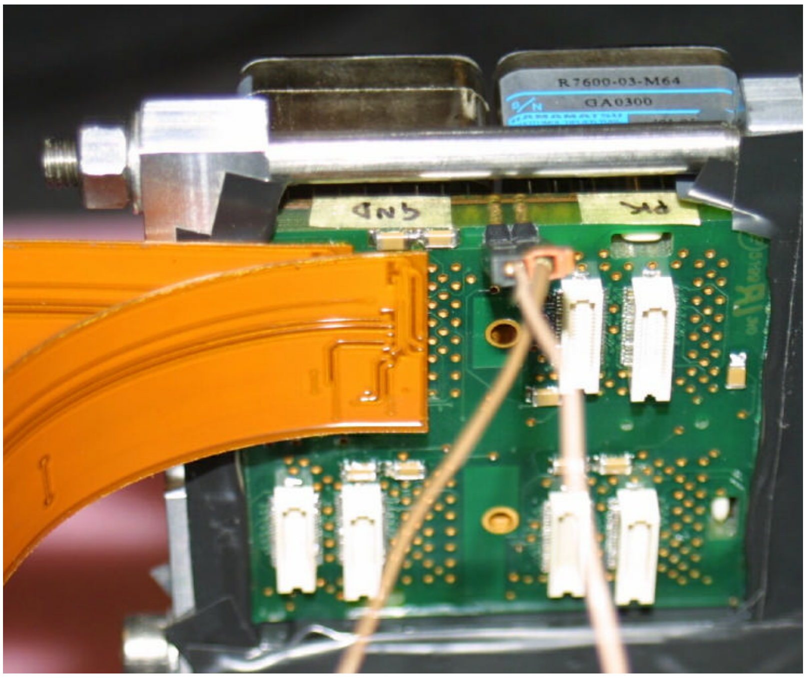

(b) The first base-board prototype: back-side view

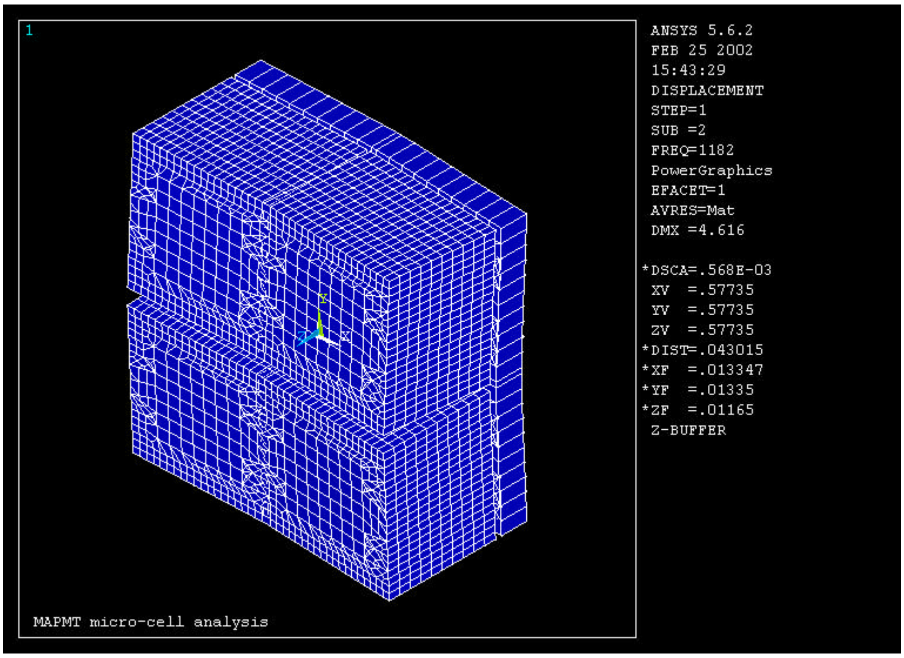

Figure 2: The displacements of the second mode of the base-board. See text

down, perhaps to 3 mm, without compromising the structural strength. The study for thickness (and, therefore, mass) reduction will be carried on whenever mode detailed information and boundary conditions will be available.

The prototype is working as expected and it is currently used in the laboratory tests for the MAPMT characterization. In this setup the MAPMT signal is amplified by means of dedicated wide-band amplifiers, connected to the base-board by means of kapton flexible cables.

4.3 Future developments

The base-board design will be possibly modified to take into account the space qualification issues. The new development should not compromise the basic design guidelines discussed above. It is not foreseen, at present, to increase the number of MAPMTs on the base-board even if this is, in principle, possible. The main reasons are due to fact that by increasing the number of MAPMTs the mechanical requirements on the base-board became tighter and the number of channels on the same PCB increase, thus making the design more complex.

The main improvements which are foreseen are the following:

- The power supplies will be changed to add a second (and possibly a third) high voltage inputs, at different voltages, on the bleeder chain chain, to save power consumption.
- The signal from the last dynode will be readout, to provide the OR of all the anodes.
- The back-side of the base-board will be modified to house the front-end chip (ASIC).

- The mounting scheme of the MAPMT will be changed to make it easier, by using a dedicated socket.

4.3.1 The ASIC

The electrical characteristics of the signals from the MAPMTs require to connect the front-end chip as close as possible to the MAPMT itself, to avoid signal degradation and interferences. The chip will be therefore housed directly on the back-side of the base-board. It is actually foreseen to realize a 64-channel chip, according to the present base-line PD design. Therefore four chips will be housed on the base-board.

A 64-channels chip will have about one hundred pins. Given the reduced space available the housing is critical. The option which minimizes the space used is the one based on the *chip on board* technology, by which the bare chip is installed. With this technology the chip must be protected by means of a suitable resin, to reduce mechanical stresses on the electrical connections as well as to protect the chip.

Alternatively a BGA package, with a pitch of 1 mm or less, can be used.

4.3.2 Interconnections

The I/O and LV connections will pass through a 1.27 mm pitch connector, allowing to connect to the macro-cell electronics by means of a flat high-density cable with 0.635 mm pitch. The number of required connections will be about eighty. The best possible location for the connector is, probably, at the center of the base-board itself. A second connector for the HV connections will be required. A possibility is provided by a small connector, with 2.54 mm pitch and four or five pins.

4.3.3 MAPMT mounting

The mounting of the MAPMTs has to be basically modified to avoid a completely hand-made installation, as it is now. First of all it has to be checked to what extent the MAPMTs pins can be directly soldered on the base-board. In any case a solution based on pass-through holes will not be applicable, because the back-side of the base-board has to house the ASICs and connectors, unless the position of the anode pins at the MAPMT exit can be substantially modified by the manufacturer. By using a surface mount housing the thickness of the base-board might be reduced, compatibly with the mechanical requirements, thus saving mass.

Assuming to avoid a direct soldering of the MAPMTs one needs a suitable socket. A prototype socket, for surface mounting, was produced [?]. A picture is shown in figure 3.

A possible assembly procedure thus can foresee the installation and test of the electronics, first, followed by the MAPMTs.

To ensure that the mechanical resistance and electrical contacts are kept all life long, the space between the MAPMT and the base-board has to be potted.

The potting has to be there in any case, to ensure the required mechanical characteristics, protection and ensure electrical insulation, even if the MAPMT were directly soldered.

The impossibility to perform a complete visual inspection can be overcome by X-ray inspection techniques and/or by defining a suitable alternative testing functional procedure, either for the MAPMT connections and for the ASICs.

The mounting described is shown in figure 4.

4.3.4 New layout

A new layout is under development, in the framework of the complete revision of the design. It foresees one voltage divider for each couple of MAPMTs.

The preliminary design is shown in figure 5.

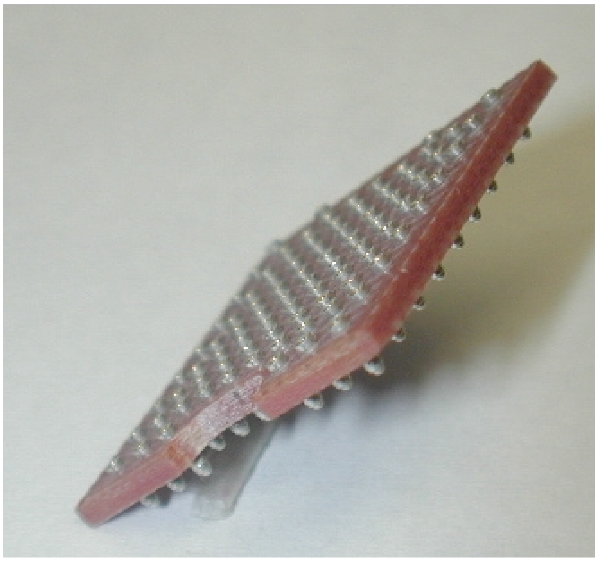

Figure 3: Prototype socket for the MAPMTs

5 Design of the PD module

A functional design of a full square module, for 6×6 MAPMTs, was carried on. Even if this geometry might not correspond to the final geometry of a module it serves as an example to guide the development process.

The design was carried on assuming, conservatively, to use a heavy optical adapter, in the form of a thick hemispherical lens, suitably shaped to remove unnecessary lens material.

The PD modules are centered and secured on the FS supporting structure via dowel pins and screws. The optical adapters, in the current design, are are fitted and glued on cells in a dye-moulded structure made of fiber-reinforced resin (e.g. cf-peek). Such a structure is centered and secured on the back-plane via dowel pins and screws.

Various drawings are shown in the following figures.

5.1 PD module: back-plane structural analysis

A static and modal analysis was performed for both a sandwich and a single piece aluminium structure of the PD module back-plane.

The picture shows the module back-plane, where concentrated masses were put to simulate the presence of micro-cells.

For the composite sandwich solution the first modal frequency is 107 Hz, and the maximum static deflection at launch is 0.2 mm. The mass is about 0.1 kg, the manufacturing is complex and cost probably high.

For the aluminium solution the first modal frequency is 141 Hz, and the maximum static deflection at launch is 0.1 mm. The mass is about 0.3 kg, the manufacturing is easy and cost probably low.

The sample PD module back-plane used for structural studies is shown in figure 7.

5.2 PD module: optical adapter support structural analysis

A FEA analysis of the optical adapter support was carried on. Any convenient thermo-plastic fiber-reinforced resin (such as gf-peek or cf-peek) was identified as viable material, also from the point

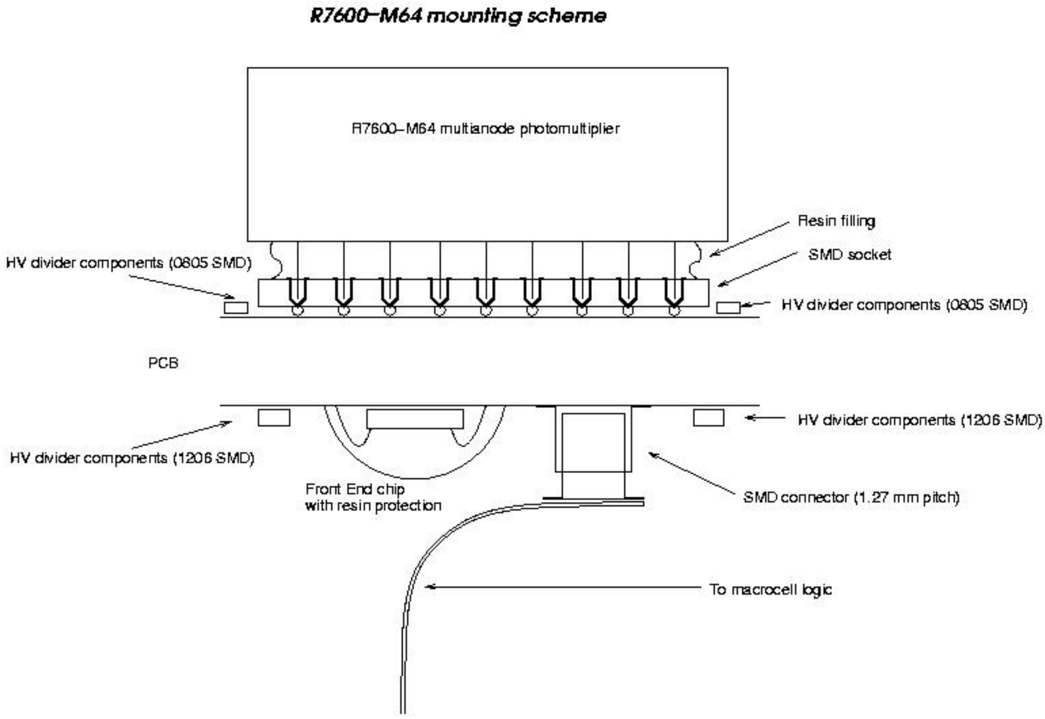

Figure 4: Scheme of the mounting scheme for the base-board (cross section)

of view of space qualification and manufacturing. A static and modal analysis was performed. The static deflection was found to be negligible. The first modal frequency is at 286 Hz.

The picture shows the supporting structure, where concentrated masses were put to simulate the presence of the optical adapter assumed to have a mass 14 g each.

The sample PD module light collection system support used for structural studies is shown in figure 8.

5.3 PD modules design for the micro-cell based layout.

Following the layout described in section 3.4.2 a possible arrangement for the PD modules was conceived. The guidelines were the following.

- To keep the (6-fold) symmetry of the design: this helps to have only a limited amount of different shapes for the modules and make the design simpler.

- As a starting point the PD modules were designed to be flat, to simplify the engineering of the PD module, by flattening any region of the FS which has been selected to host one module. The alternative option to leave the PD module curvature as required by the FS shape, more complex from the engineering point of view, can be considered if the resulting fitting to the FS is not good enough.

- The dimensions of the PD modules should be compatible with the choice to flatten the PD modules. Therefore a maximum dimension of the PD module limited to about ten micro-cells was chosen. This value seems to be a good compromise from structural requirements point of view as the modules are not too massive.

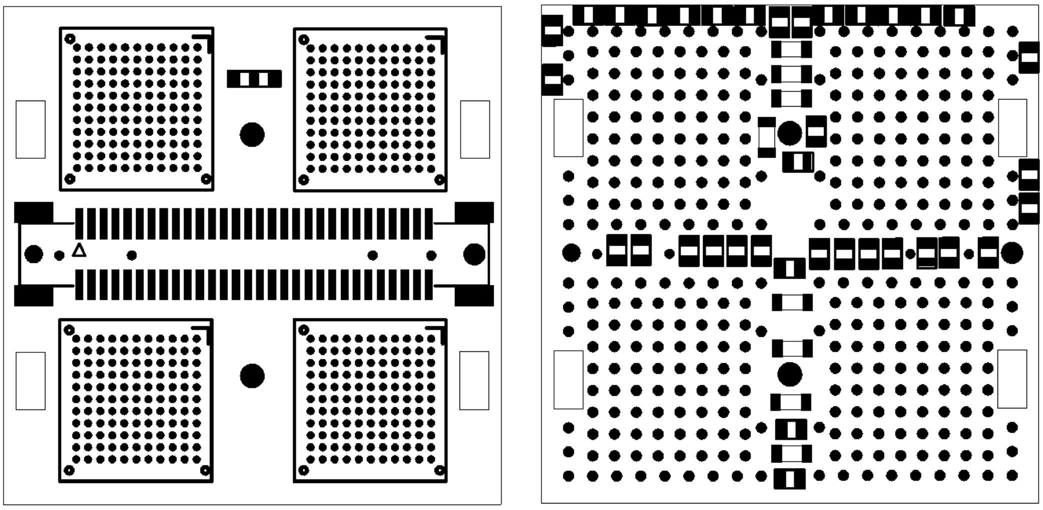

Figure 5: Scheme of the new layout of the micro-cell base-board.

One possible layout, following the previous assumptions, was conceived, In figure 9 one-third of the FS is shown, with the PD modules layout for half of it. All others modules can be built form the ones shown in figure, possibly by mirroring the shape. Therefore, in total, nineteen module shapes have to be realized, or twenty-six, if one considers mirror shapes as basically different.

However if one accepts to make the design more complex by allowing curved modules, the dimensions of the modules are only limited by the engineering issues (mainly structural). In this way the number of basically different shapes can be reduced by using larger modules.

6 PD budgets

6.1 Mass

The December 2000 accommodation study quoted an overall PD mass of 700 kg, while in the pre-phase A Genova report the overall mass of the PD, as defined at the beginning of the present report, is estimated to be about 750 kg. A more detailed breakdown of the mass of the different components is show in the table below 10. It was prepared by using rather conservative assumptions, on some items. The interval between minimum and maximum values is sometimes due to different possible alternative choices, e.g. for the optical adapters and for the choice of the materials in various items. The layout number three was assumed as a baseline and, for the purpose of calculation, an average module was defined.

The estimation of the mass of sensors, optical adapters, micro-cells and modules as well as electronics boards was based on the functional design discussed in the present note.

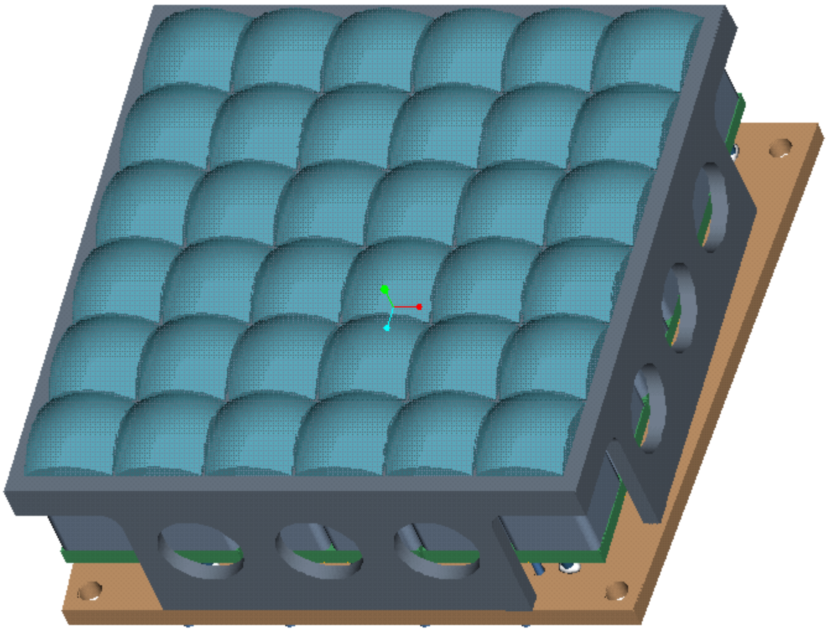

(a) PD module, front view of the assembled module.

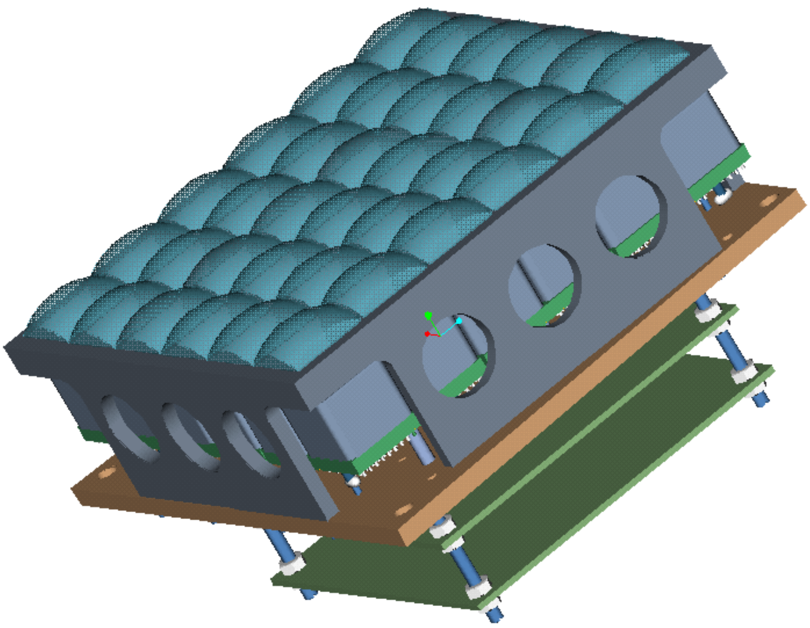

(b) PD module, side view of the assembled module.

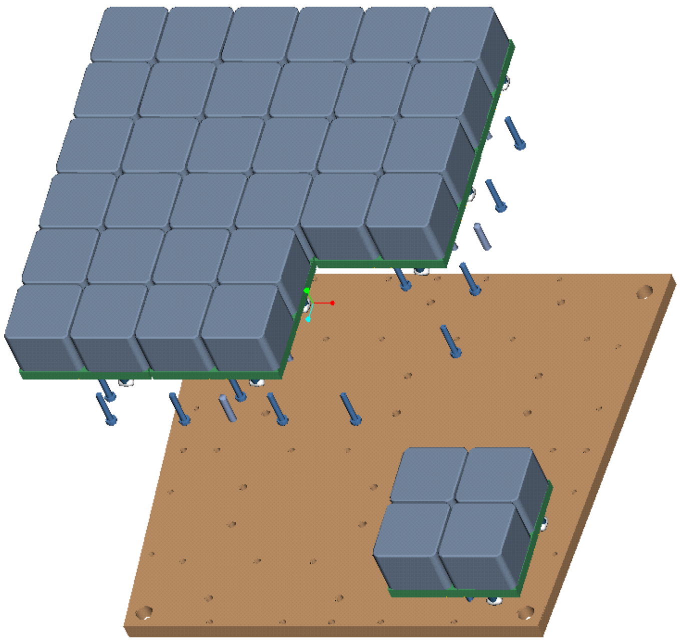

(c) PD module, view of the micro-cells installation onto the back-plane module.

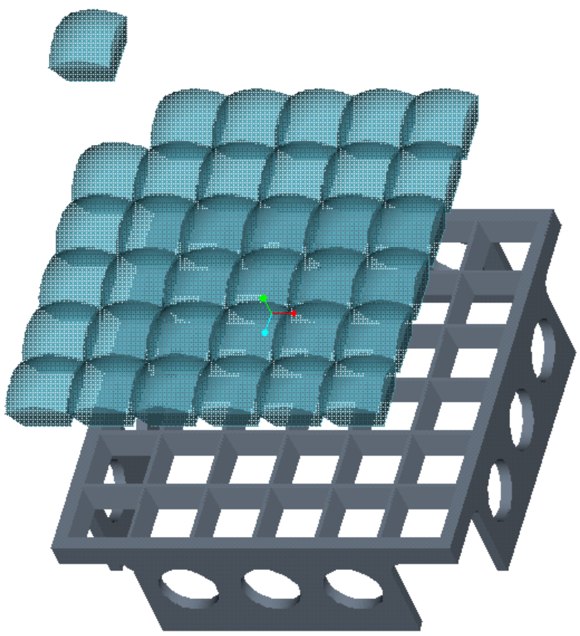

(d) PD module, exploded view of the optical adapters supporting structure.

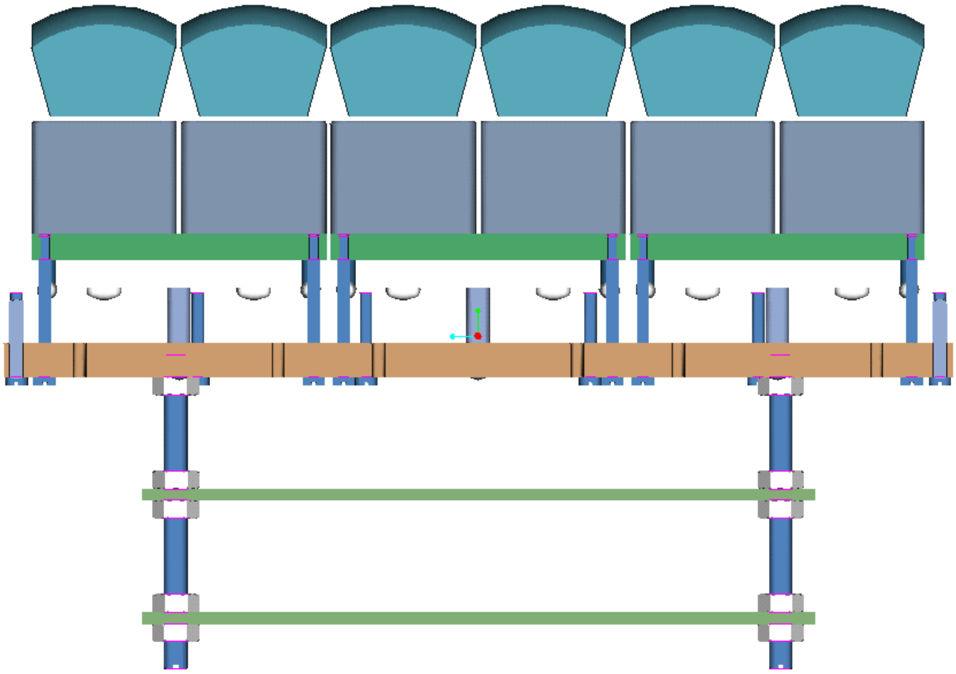

(e) PD module, one side view of the assembled module.

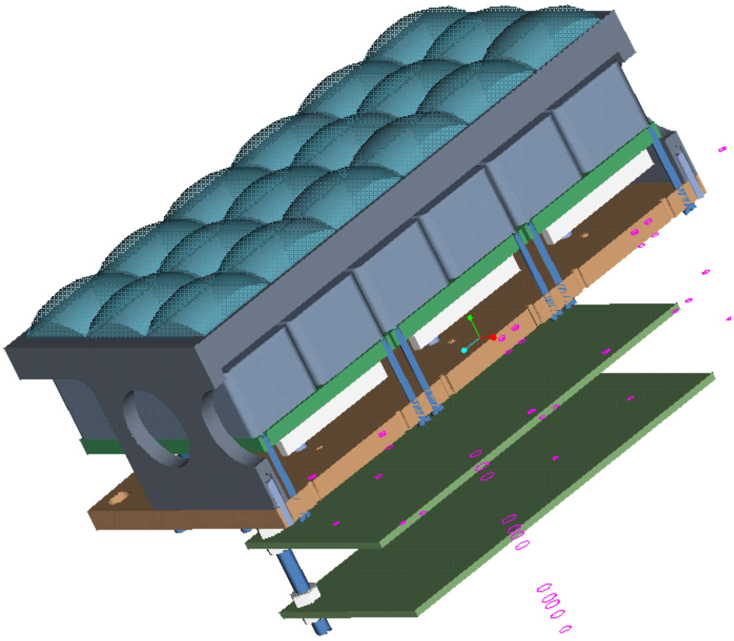

(f) PD module, one more side view of the assembled module.

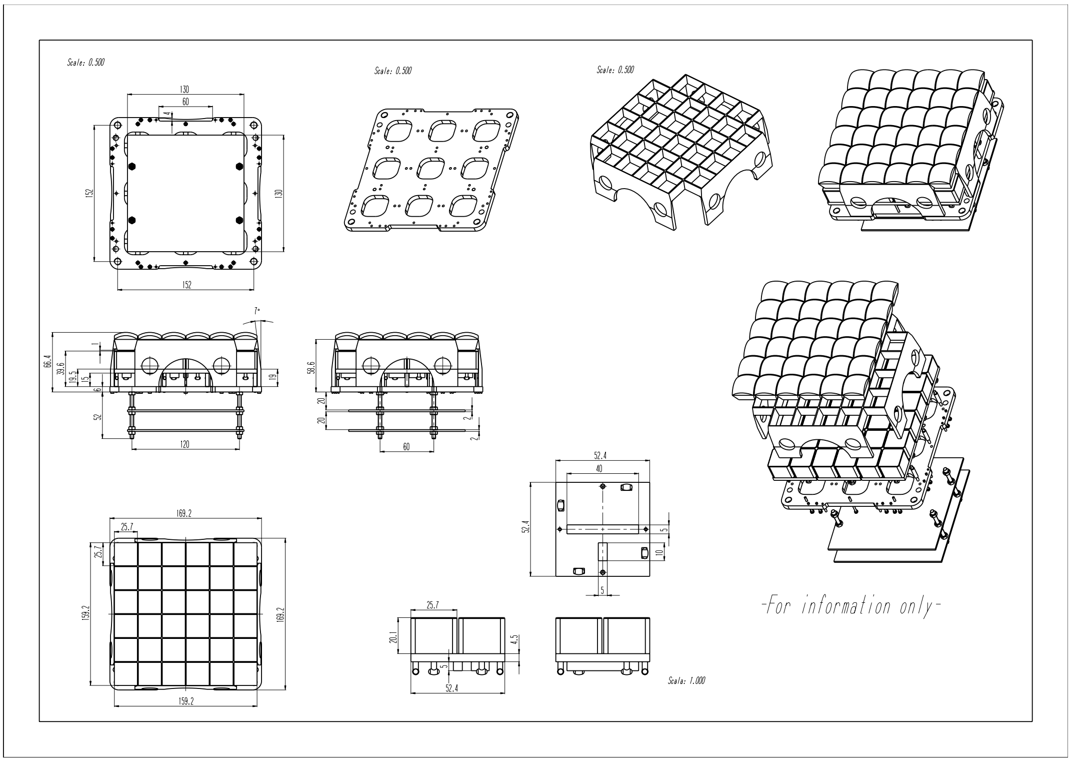

Figure 6: PD module, quoted views.

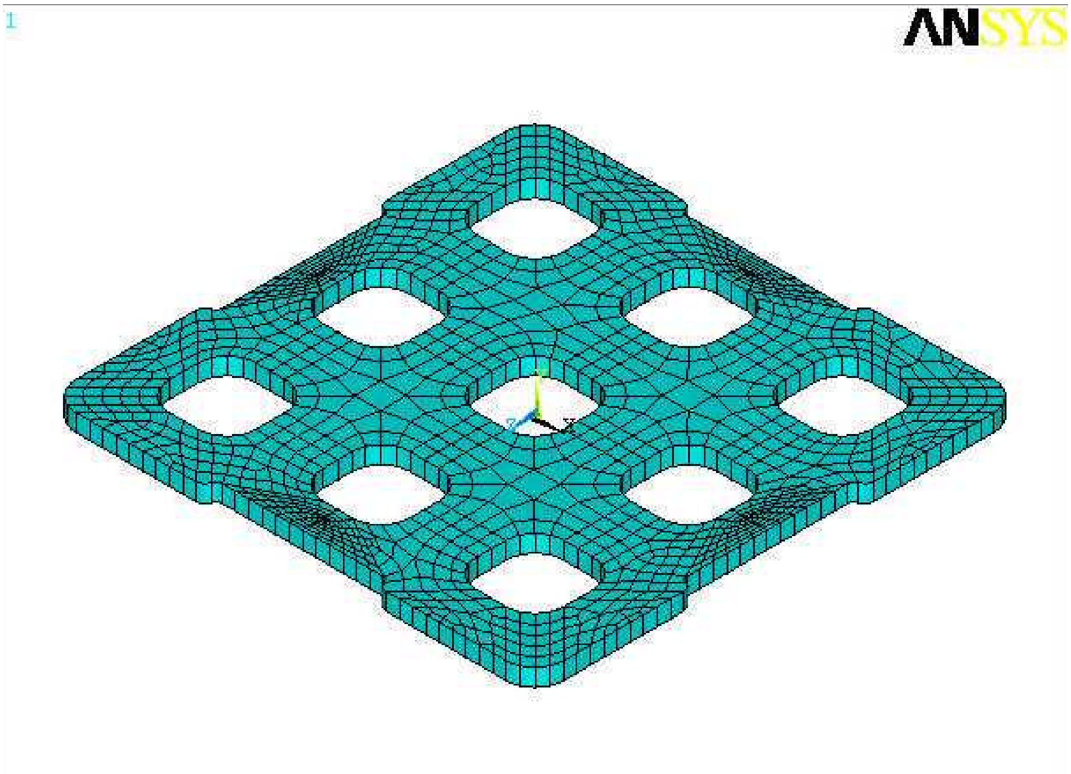

Figure 7: View of the sample PD module back-plane for structural studies.

6.2 Power consumption

6.2.1 MAPMTs

The required MAPMT power consumption, tuned on the expected background levels with the standard procedure, is only dependent on the overall FS area, and not on its segmentation.

The light flux entering the EUSO Instrument, from a given uniform and isotropic light flux B, is given by:

$$\frac{B D_{\mathrm{EP}}{}^{2} \pi^{2} \sin\gamma^{2}}{4} \quad . \tag{6.1}$$

The overall rate of the photons detected on all the FS is therefore given by the relation:

$$\frac{B D_{\mathrm{EP}}{}^{2} \pi^{2} \sin\gamma^{2}}{4} \varepsilon_{\mathrm{OPT}} \varepsilon_{\mathrm{DET}} \quad , \tag{6.2}$$

where $\varepsilon_{\mathrm{OPT}}$ and $\varepsilon_{\mathrm{DET}}$, are, respectively, the overall light transmission of the optics and the overall detection efficiency of the photo-detector. Assuming $\varepsilon_{\mathrm{OPT}} = 0.5$, $\varepsilon_{\mathrm{DET}} = 0.15$ and $B \approx 3 \cdot 10^{11}$photons$\cdot$ m^{-2}s^{-1}str^{-1} one gets an overall rate of $5.5 \cdot 10^4$ MHz equivalent to about 10 MHz per single MAPMT.

Based on previous studies, a power consumption of about 150 W for the MAPMTs alone can be considered by using a suitable powering scheme [3, 2].

6.2.2 Front-end, macro-cell and trigger electronics

For the purpose of thermal studies only, an average power consumption of 2 mW per channel, by the front-end electronics alone, will be assumed. The overall power consumption of the macro-cell and trigger electronics, as well as the central control unit can be estimated in the range of 200 W.

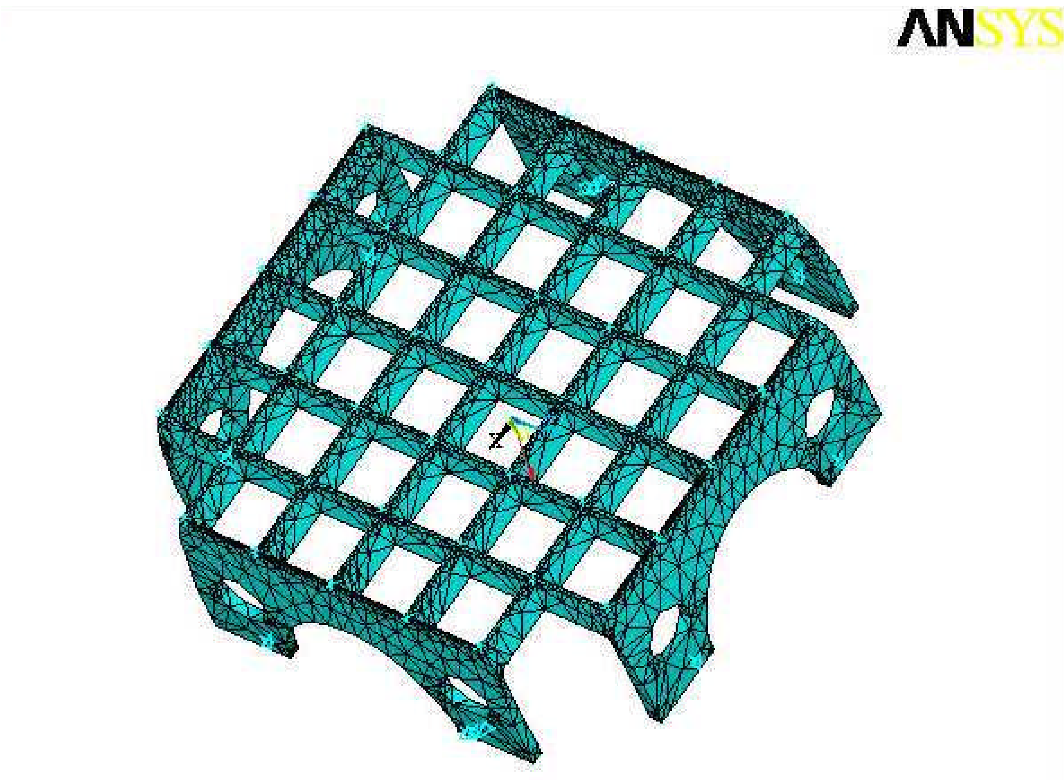

Figure 8: View of the sample PD module light collection system support for structural studies.

7 Critical items

In addition to the specific items mentioned for the new M16F the following general items must be considered.

- MAPMT aging: operate the MAPMT at low gain to reduce aging as the real amount of light the MAPMT will receive on orbit is, to some extent, uncertain. Moreover the possibility to increase the HV during the mission to recover a possible gain decrease must exist.

- MAPMT: Voltage divider optimization and power consumption minimization (non resistive voltage dividers?).

- HV/LV design. Evaluate the need for buffering batteries:

  - ISS does not guarantee power availability at any time, only average values.
  - increase the effective power available to the electronics by exploiting the short observation duty cycle ? Is it compatible with the thermal control of the FS.

  Up to 40 W h/kg space qualified batteries are normally used in satellites.

- Evaluate the environmental susceptibility.

- Overall mass reduction.

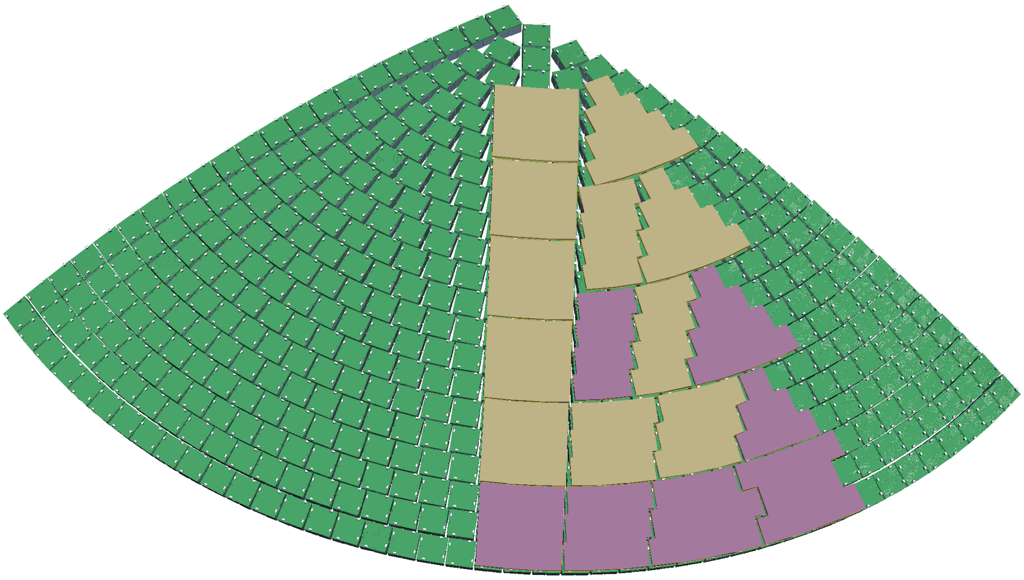

Figure 9: One-third of the FS, with the PD modules layout.

7.0.3 FS protection

One important critical item is related to the fact that a connection of the MAPMTs in negative polarity (i.e. with cathode at a large negative potential) is assumed. This is mainly for the following reasons:

- to save space on the front-end electronics side by avoiding one high-voltage capacitor per channel;
- to improve safety on the front-end electronics side in case of high-voltage capacitor failure.

The problem induced by this setup is that the FS is now at a large negative potential, in an environment with a significant plasma concentration. This might cause charge buildup on the focal surface as well as electrons and ions acceleration.

This problem can be limited by installing a protection grid just in front of the FS. Gold-plated tungsten grids, with an optical transparency as large as 0.98 are available and have been used in space applications [1].

References

[1] Primo Attinà, Alenia Spazio, private communication.

[2] Gregorio Landi, HV-LV distribution in EUSO, internal EUSO-Firenze note.

[3] M. Ameri et al., *Study report on the EUSO photo-detector design*, Report INFN/AE-01/04, available at http://wwwsis.lnf.infn.it/pub/INFN/AE-01/04.pdf, 06/04/2001.

[4] Saft Alcatel Space, "`http://www.saft.alcatel.com/space/`".

	#	MASS for ONE MODULE			TOTAL MASS for PD		
ITEM	#	MIN(g)	AVE(g)	MAX(g)	MIN(kg)	AVE(kg)	MAX(kg)
MAPMT	36.000	1044	1044	1044	161	161	161
Base-board (2x2) plus components	9.000	306	306	306	47	47	47
Back-plane	1.000	35	153	270	5	23	42
Lenses / Light pipes / RIKEN optical adapter	36.000	179	486	793	28	75	122
Lenses support	1.000	210	240	270	32	37	42
Signal connectors (BB to EB1)	18.000	360	360	360	55	55	55
Ancillary connectors (BB to EB2) (HV/LV/...?)	18.000	360	360	360	55	55	55
Signal cables (BB to EBx)	9.000	135	135	135	21	21	21
Ancillary cables (BB to EBx) (HV/LV/...?)	9.000	270	270	270	42	42	42
Electronics board 1: RO/C ELE (EB1)	1.000	173	230	288	27	35	44
Electronics board 2: HV/LV (EB2)	1.000	173	230	288	27	35	44
Signal connectors (EB1 to CDH)	1.000	20	20	20	3	3	3
Ancillary connectors (EB2 to CDH)	1.000	20	20	20	3	3	3
Signal cables (Ebx to CDH)	1.000	15	15	15	2	2	2
Ancillary cables (Ebx to CDH)	1.000	100	100	100	15	15	15
Screws and other mechanical stuff	1.000	150	150	150	23	23	23
D f/e electronics + potting (ASIC)	36.000	108	108	108	17	17	17
A f/e electronics + potting (ASIC)	9.000	45	45	45	7	7	7
HV power supplies (x2 redundancy)	0.006	32	32	32	5	5	5
LV power supplies (x2 redundancy)	0.006	65	65	65	10	10	10
Buffer batteries	0.006	65	65	65	10	10	10
Addtional harness	1.000	100	100	100	15	15	15
MAPMTs potting	1.000	80	120	160	12	18	25
Other pottings	0.006	130	130	130	20	20	20
CONTINGENCY: included in each item		0	0	0	0	0	0

Figure 10: Mass breakdown of the FS components.